

Compositional trends in aeolian dust along a transect across the southwestern United States

Harland L. Goldstein,¹ Richard L. Reynolds,¹ Marith C. Reheis,¹ James C. Yount,¹ and Jason C. Neff²

Received 12 January 2007; revised 8 June 2007; accepted 21 September 2007; published 14 March 2008.

[1] Aeolian dust strongly influences ecology and landscape geochemistry over large areas that span several desert ecosystems of the southwestern United States. This study evaluates spatial and temporal variations and trends of the physical and chemical properties of dust in the southwestern United States by examining dust deposited in natural depressions on high isolated surfaces along a transect from the Mojave Desert to the central Colorado Plateau. Aeolian dust is recognized in these depressions on the basis of textural, chemical, isotopic, and mineralogical characteristics and comparisons of those characteristics to the underlying bedrock units. Spatial and temporal trends suggest that although local dust sources are important to the accumulated material in these depressions, Mojave Desert dust sources may also contribute. Depth trends in the depressions suggest that Mojave sources may have contributed more dust to the Colorado Plateau recently than in the past. These interpretations point to the important roles of far-traveled aeolian dust for landscape geochemistry and imply future changes to soil geochemistry under changing conditions in far-distant dust source areas.

Citation: Goldstein, H. L., R. L. Reynolds, M. C. Reheis, J. C. Yount, and J. C. Neff (2008), Compositional trends in aeolian dust along a transect across the southwestern United States, *J. Geophys. Res.*, *113*, F02S02, doi:10.1029/2007JF000751.

1. Introduction

[2] Atmospheric mineral dust, once deposited, affects physical and ecological landscapes in several ways. Clear examples are thick, widespread, and fertile loess deposits consisting entirely of wind-deposited sediment, primarily composed of silt [e.g., Pye, 1984]. Dust infiltration into surficial deposits and soils may strongly alter the texture and structure of surficial materials, thereby influencing development of landscapes, soil fertility, and soil hydrology. Whereas dust deposition on surfaces over a long time period is capable of producing potentially very stable landforms, such as desert pavement [McFadden *et al.*, 1986, 1987], it may also deliver essential plant nutrients to disparate ecosystems in different climatic settings, including tropical forests [Swap *et al.*, 1992; Chadwick *et al.*, 1999; Vitousek *et al.*, 1999, 2003], drylands [Yaalon and Ganor, 1973; Neff *et al.*, 2005; Reynolds *et al.*, 2006a], and alpine tundra [e.g., Muhs and Benedict, 2006]. The atmospheric addition of fines (silt and clay) to soils in these and other settings may also affect water infiltration and soil moisture capacity [McDonald *et al.*, 1995, 1996; McFadden *et al.*, 1998; Reynolds *et al.*, 2006b].

[3] Assessments of the influence of dust on ecosystems generally rely on recognition of the dust component in soils compared to material otherwise derived from regolithic weathering or other local sources. In many settings, these dust components make up a relatively small proportion of the surficial material [e.g., Chadwick *et al.*, 1999; Reynolds *et al.*, 2006a, 2006b]. Our approach involves the study of dust captured in isolated natural dust traps, such as potholes, rock crevices, and cavities, including vugs in volcanic rocks [Reheis *et al.*, 2002]. Much of the fine-grained sediment in these types of traps may have been introduced as dust, the evidence for which consists of large differences in texture, chemistry, and mineralogy between the trapped surficial sediment and bedrock [Reynolds *et al.*, 2006c].

[4] The presence of relatively high abundances of dust in natural traps offers the opportunity to address the influences of deposited dust on the landscape geochemistry of drylands over areas spanning regions and ecosystems. The spatial variations in dust composition are likely related to local sources and (or) sorting processes over long distances in the atmosphere. Temporal variations in dust composition may reflect changes in source areas and (or) environmental conditions at the source area, whether forced by natural or land-use conditions.

[5] The purpose of this study is to examine compositional variations of mineral dust deposited during the past few centuries in isolated natural dust traps spanning a region from the Mojave Desert of southern California to the central Colorado Plateau (Figure 1). The Mojave Desert contains many dust sources and sinks [e.g., Muhs, 1983; Wilshire, 1980; Gill, 1996; Reheis and Kihl, 1995; Reheis *et al.*,

¹Denver Federal Center, U. S. Geological Survey, Denver, Colorado, USA.

²Geological Sciences and Environmental Studies Departments, University of Colorado, Boulder, Colorado, USA.

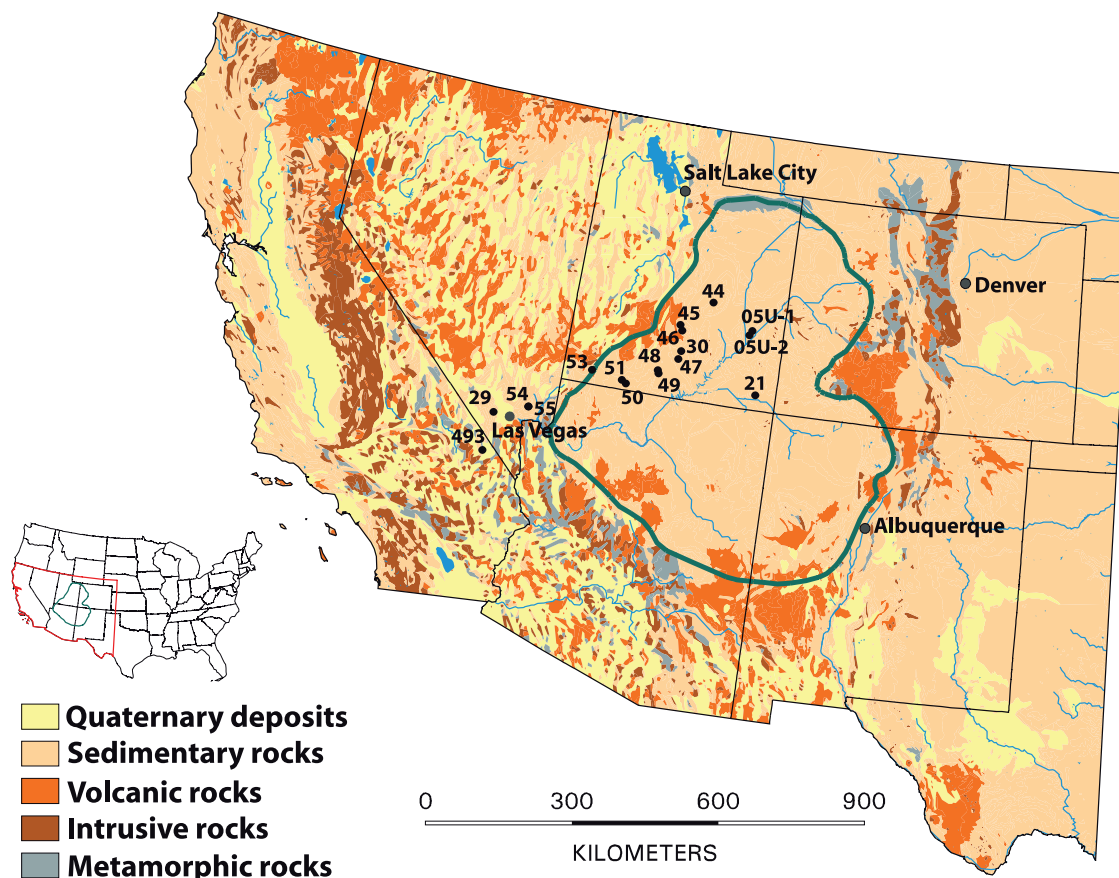


Figure 1. Generalized geologic map of the southwestern United States showing the southwest-northeast transect of the sampled pothole sites (small closed circles). The transect runs from the Mojave Desert to the central Colorado Plateau. Green outline denotes the boundary of the Colorado Plateau. Sites 54 and 55 are in close proximity and are displayed as one point.

2002; *Reheis*, 2006]. Dust plumes originating from the Mojave Desert may be generated by winds from any direction. One major dust pathway, driven by west-southwesterly winds related to late winter–early spring frontal storms, is from the central Mojave Desert onto the southwestern edge of the Colorado Plateau, as documented by regional-scale satellite images [*Chavez et al.*, 2002; *Reynolds et al.*, 2003]. The central Colorado Plateau has a long history of dust accumulation [*Reheis et al.*, 2005; *Reynolds et al.*, 2006b]. These sets of observations led to the hypothesis that at least some of the dust sequestered in central Colorado Plateau surficial deposits was derived from the Mojave Desert, and the current study was designed to test this hypothesis. It was not our objective to identify specific dust sources for, or to determine the amount of, Mojave Desert dust in Colorado Plateau soils, because of the multitude of known and potential sources, both local and distant [*Reynolds et al.*, 2001a, 2006a, 2006b] and because of the known variety of dust sources in the Mojave and southern Great Basin deserts [e.g., *Reheis*, 2006] (<http://esp.cr.usgs.gov/info/dust/inventory/>).

[6] One topic of this study centers on dust contributions to potential plant nutrients. Potential plant nutrients are elemental nutrients present in the sediment that may or may not be available for biogeochemical processes. A

pattern of potential nutrients in surficial deposits, if found to be associated with dust, would elucidate the influence of a major dust source region on landscape fertility with increasing distance from that source area. The possibility that dust from outside the Colorado Plateau might help fertilize parts of the Plateau has added interest because old clastic sedimentary rocks that underlie large areas of the Plateau are relatively nutrient-poor, notably mature sandstones having their origins as sand dune fields. Thus, relatively modest dust fall onto these areas might have a disproportionately large effect on soil fertility [*Neff et al.*, 2006; *Reynolds et al.*, 2006a]. A lack of a spatial pattern in potential nutrients would reveal instead the importance of mostly local to subregional contributions.

2. Regional Setting

[7] The study area is defined by a transect of sampling sites on mostly sandstone from the eastern Mojave Desert in southeastern California to the central Colorado Plateau in Utah (Figure 1; Table 1). In general, the geologic and physiographic complexity of the study region decreases from the Mojave Desert to the Canyonlands province of the central Colorado Plateau (<http://mojave.usgs.gov/rvde/>) [*Graf et al.*, 1987; *Patton et al.*, 1991; *King and Beikman*,

Table 1. Pothole Site Location Information

Sample Site	Latitude ^a	Longitude ^a	Elevation, ^b m	Location	Formation	Geologic Map Reference
44	38.8622	-110.8369	2188	San Rafael Swell, Utah	Navajo Sandstone	<i>Williams and Hackman</i> [1983]
45	38.3607	-111.5304	2510	Bicknell, Utah	Navajo Sandstone	<i>Williams and Hackman</i> [1983]
46	38.2601	-111.4597	2262	Teasdale, Utah	Navajo Sandstone	<i>Williams and Hackman</i> [1983]
47	37.7363	-111.4414	1818	Escalante, Utah	Navajo Sandstone	<i>Hackman and Wyant</i> [1973]
48	37.4726	-111.8749	2046	GSENM, Utah ^c	Entrada Sandstone	<i>Hackman and Wyant</i> [1973]
49	37.4199	-111.8497	1859	GSENM, Utah ^c	Navajo Sandstone	<i>Hackman and Wyant</i> [1973]
50	37.1322	-112.5633	1690	Kanab, Utah	Navajo Sandstone	<i>Eppinger et al.</i> [1990]
51	37.1897	-112.6646	1801	Mt. Carmel Junction, Utah	Carmel Limestone	<i>Eppinger et al.</i> [1990]
53	37.2704	-113.3988	1455	Leeds, Utah	Navajo Sandstone	<i>Eppinger et al.</i> [1990]
54	36.3874	-114.6863	906	Buffington Pocket, Nevada	Aztec Sandstone (redbed) ^d	<i>Bohannon</i> [1978]
55	36.3867	-114.6870	855	Buffington Pocket, Nevada	Aztec Sandstone (redbed) ^d	<i>Bohannon</i> [1978]
29	36.1664	-115.4522	1345	Red Rocks, Nevada	Aztec Sandstone (redbed) ^d	<i>Page et al.</i> [2005]
30	37.8904	-111.4067	1984	Boulder, Utah	Navajo Sandstone	<i>Hackman and Wyant</i> [1973]
05U-1	38.4501	-109.8169	1782	Island in the Sky, Utah	Navajo Sandstone	<i>Williams</i> [1964]
05U-2	38.3668	-109.8667	1879	Island in the Sky, Utah	Navajo Sandstone	<i>Williams</i> [1964]
21	37.2934	-109.5354	1421	Bluff, Utah	Bluff Sandstone	<i>Haynes et al.</i> [1972]
493	35.4387	-115.5195	1615	Mescal Range, California	Aztec Sandstone (redbed) ^d	<i>Jennings</i> [1961]

^aLatitude and longitude displayed in NAD83 datum.

^bElevation determined from 30 m DEM.

^cGSENM refers to Grand Staircase Escalante National Monument.

^dRedbeds contain fine-grained hematite as grain coatings.

1974]. The sampling area in the eastern Mojave Desert is characterized by mountain ranges of a wide variety of lithic types that are commonly flanked by sparsely vegetated alluvial fans and valley floors that include mostly dry river beds as well as dry lake beds. In contrast, much of the Colorado Plateau is characterized by high-elevation, nearly flat-lying Paleozoic and Mesozoic sedimentary rocks, separated by broad upland valleys (such as Monument Valley) or deeply incised by canyons as in Canyonlands [Hunt, 1956]. Igneous rocks occupy only small areas of the central Colorado Plateau and comprise mainly middle Tertiary, intermediate-composition (trachyte and trachyandesite) intrusions of the La Sal, Abajo, and Henry Mountains [Nelson and Davidson, 1998]. Thick sequences of Tertiary lavas, dominantly basaltic in composition [Luedke and Smith, 1978] occur discontinuously along the western and southwestern margins of the Colorado Plateau [see Patton *et al.*, 1991]. Andesitic to dacitic and rhyolitic rocks of the middle Tertiary San Juan and Marysvale volcanic fields border the respective eastern and western margins of the Colorado Plateau [e.g., Rowley *et al.*, 1998; Lipman, 2000].

3. Field and Laboratory Methods

[8] The sediments for this study were collected from natural depressions (potholes) that weathered into mostly Jurassic aeolian sandstones (Table 1). The sampled potholes are topographically isolated, so that sediment in them can have only two sources, airborne dust and detritus derived from the immediately surrounding catchment of the sandstone surface. The surface area of individual potholes and their catchments ranged from about 0.5–1.0 m² and 50–100 m², respectively. In this study we avoided sites with highly friable bedrock that could shed large amounts of detritus into potholes, thereby diluting the dust accumulations. However, all sampled potholes contained some local sediment as revealed primarily by sand content. Each pothole was sampled incrementally by depth. Three sediment samples were taken with a trowel from each pothole

(typically at depths of 0–1 cm, 1–2 cm, and 2–5 cm). For each sample, about 50 g of fine-grained material was obtained over an area of 500–1000 cm². A sample of the bedrock in which the pothole formed was also collected. Pothole elevations were determined from 30-meter digital elevation models (National Elevation data set, available at <http://seamless.usgs.gov>).

[9] Biologic soil crust (BSC) that typically forms on the pothole-filling sediment makes an excellent trap for dust [Reynolds *et al.*, 2001a], enabling dust sequestration over a long time period as the growth of BSC keeps pace with slowly accumulating sediment. Most sampling sites were associated with mature BSC, including lichen and cyanobacteria. The presence of mature BSC on the surface of pothole sediment (ca. 0–1 cm depth) indicates stability over many decades, on the order of 50–70 years [Belnap, 1993]. Therefore, dust in the pothole-filling sediment, typically as much as 10 cm thick, probably represents accumulation over at least several centuries [Belnap, 1993; Reynolds *et al.*, 2001a]. The temporal framework based on the presence of mature BSC follows previous studies by Reheis *et al.* [2002] and Reynolds *et al.* [2006c] on dust deposited in comparable settings (vugs in volcanic rocks and potholes) likely during the last few hundred years.

[10] To assess variations and trends in physical and chemical parameters, sediment was analyzed for particle size, CaCO₃ content, magnetic properties, and bulk chemistry. Particle-size analysis (PSA) was performed on the <2-mm size fraction of the surficial sediment and on bedrock using a Malvern particle size laser analyzer. Bedrock samples were disaggregated by pounding the samples lightly using a mortar and pestle. The pounding, along with the pretreatments (discussed below), were the best methods to obtain a bedrock PSA sample most representative of the fundamental grain size. Prior to PSA analysis, all samples were prepared by digesting organic matter and CaCO₃ using 30% H₂O₂ and 15% HCl, respectively, and sodium hexametaphosphate was added to each sample to deflocculate clays. Such pretreatment could affect the natural aggregation and thus size

fraction of the pothole sediment; however, low calcium carbonate content in these sediments suggests that such an effect is likely minimal. Calcium carbonate content was measured using a Chittick apparatus as described by *Machette* [1986] whereby 6N HCl is applied to the sample and the gas evolved from the reaction is used to calculate the amount of calcium carbonate.

[11] Magnetic properties were determined on both <2-mm and <63- μm size fractions of the pothole samples as well as on bulk bedrock samples. Magnetic susceptibility (MS) was measured in a 0.1 mT induction at a low frequency of 600 Hz (MS_{lf}) and high frequency of 6000 Hz (MS_{hf}) using a susceptometer with a sensitivity better than about $4 \times 10^{-7} \text{ m}^3/\text{kg}$. Using an impulse magnetizer, isothermal remanent magnetization (IRM) was first imparted in a 1.2T induction ($\text{IRM}_{1.2\text{T}}$) and then in the opposite direction using an induction of 0.3T ($\text{IRM}_{0.3\text{T}}$). Measurements of IRM were made using an Agico high-speed spinner magnetometer. Values of $\text{IRM}_{0.3\text{T}}$ and MS are highly correlated ($r^2 = 0.97$) indicating that ferrimagnetic magnetite dominates the MS signals, as found by *Reynolds et al.* [2006c] for a similar but smaller set of sediment samples from sites in the Mojave Desert to the west of the current study area. Because $\text{IRM}_{0.3\text{T}}$ avoids the effects of paramagnetism and diamagnetism on MS [*Evans and Heller, 2003*] values of $\text{IRM}_{0.3\text{T}}$ were taken as the estimate of magnetite abundance. Hard isothermal remanent magnetization (HIRM), a measure of hematite content, was calculated as $(\text{IRM}_{1.2\text{T}} + \text{IRM}_{0.3\text{T}})/2$. The S parameter was calculated as $(\text{IRM}_{0.3\text{T}}/\text{IRM}_{1.2\text{T}})$ and indicates the relative amount of strongly magnetic material (e.g., magnetite) to all magnetic material (e.g., magnetite plus hematite). Values of S close to 1 indicate high relative amounts of magnetite. Confirmation of magnetic mineralogy was done with reflected-light petrographic identification of magnetic grains separated from bulk samples [*Reynolds et al., 2001b*] and polished in epoxy mounts.

[12] Dust (<63 μm) and bedrock samples were analyzed for chemical constituents by inductively coupled plasma-atomic emission spectrometry (ICP-AES) and inductively coupled plasma-mass spectrometry (ICP-MS) techniques [*Lichte et al., 1987*].

[13] Strontium isotopes (^{87}Sr and ^{86}Sr) were measured on the fine fraction and sand fraction of the pothole surface sediment, as well as on bulk bedrock at each site. In addition, one sample of basalt collected near site 45 was also analyzed for Sr isotopes. Strontium isotopes were measured on both the labile and residual fractions. Labile fractions were separated by leaching samples in 5 M acetic acid to obtain the acid soluble carbonate fraction and the leachate was centrifuged and purified with conventional ion-exchange methods. The residue that was not dissolved by the acetic acid leach was rinsed repeatedly with distilled water and dried. This residue was then dissolved using various mineral acids until the sample was completely in solution and was then purified using conventional cation ion-exchange methods. Leach and residue fractions were loaded separately on single tantalum filaments with phosphoric acid. Total chemistry and loading blanks were <200 pg and, therefore, negligible. Isotope ratios were measured with an automated VG54 sector multi-collector, thermal ionization mass spectrometer in dynamic mode. Mass dependent fractionation was corrected assuming an $^{86}\text{Sr}/^{88}\text{Sr}$ of 0.1194.

Sr isotope ratios are reported relative to SRM-987 standard value of 0.71025.

4. Results

4.1. Magnetic Properties and Petrographic Observations

[14] Magnetic data and petrographic observations indicate that magnetic minerals are much more abundant in the pothole sediments than in associated bedrock. Magnetite is common in all sediment samples ($\text{IRM}_{0.3\text{T}}$ ranges from 1.85 to $17.1 \times 10^{-3} \text{ Am}^2 \text{ kg}^{-1}$; in contrast, $\text{IRM}_{0.3\text{T}}$ values of underlying sandstone are all less than $2.0 \times 10^{-4} \text{ Am}^2 \text{ kg}^{-1}$) (Figure 2). Similarly, on the basis of HIRM values, hematite concentrations in the sediment are much greater than in the bedrock (Figure 3).

[15] Petrographic observations of magnetic-mineral extracts from pothole surface sediment confirm the presence of magnetite and hematite and provide information about their origins. The magnetic mineral extracts consist mainly of strongly magnetic magnetite and titanomagnetite. These minerals are commonly intergrown with hematite, ilmenite, pseudobrookite, and ilmenorutile. Such Fe-Ti oxide minerals originally formed in igneous rocks, and their associations are typical of those produced during initial cooling [*Haggerty, 1976*]. The magnetite and titanomagnetite, along with closely associated Fe-Ti oxides, are typically about 1–30 μm in diameter, although some are as large as about 50 μm . Fragments of igneous rocks (apparently derived from basalt on the basis of texture) are also present in some samples and contain abundant, small ($\leq 1 \mu\text{m}$) Fe oxides, probably magnetite. The uppermost (0–1 cm depth) samples at many sites also contain rare, small silt size (<20 μm), spherical magnetic particles, mostly consisting of magnetite but probably including other Fe oxides. On the basis of their shape and characteristic internal texture, these particles are identified as fly ash produced via coal combustion [*Lauf, 1982; Lauf et al., 1982*]. Small fragments of steel are also found in the BSC. All such anthropogenic grains are absent in sediment beneath the biologic soil crust. Strongly magnetic magnetite and titanomagnetite are essentially absent in the associated bedrock. The few occurrences in bedrock consist of rare magnetite inclusions within sand-size quartz grains.

[16] The spatial distributions of magnetite ($\text{IRM}_{0.3\text{T}}$) and hematite (HIRM) show regional patterns (Figures 2 and 3). Magnetite abundance is highest in the western sites with overall gradual decrease toward the east. This trend of diminishing magnetite content is broken by moderate increases in $\text{IRM}_{0.3\text{T}}$ values in sites 47, 30, 46, and 45. Of the sites located on the Colorado Plateau, these are close to basaltic bedrock at the western margin of the Colorado Plateau (Figure 1) and thus may have received additional magnetite from local basaltic sources. The spatial pattern for hematite abundance does not track magnetite abundance, except that hematite contents are highest in western sites (Figure 3). Hematite abundance is also high in the easternmost sites in the Canyonlands province where magnetite contents in the pothole sediments are uniformly low. These sites lie amongst widespread red sedimentary rocks (redbeds) in which the red colors are produced by very fine-grained hematite as grain coatings. Hematite abundance is low at sites 48, 30, 46, 45, and 44 (from west to east). The

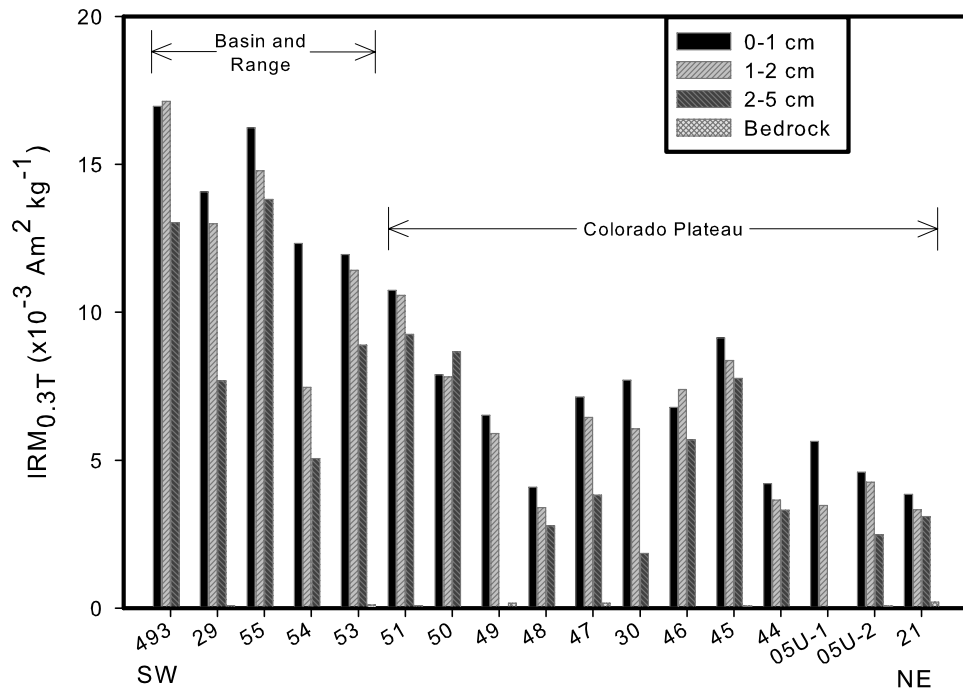


Figure 2. Bar plot of $IRM_{0.3T}$ (magnetite) for pothole sediment and underlying bedrock. Magnetite content decreases to the northeast and is much more abundant in the sediment samples than in the associated bedrock. Bedrock at all sample sites (except 46 and 05U-1) are included in the plot and are very small values compared to pothole sediment.

relative amounts of magnetite and hematite (expressed by the S-parameter) also show a broad spatial distribution, with highest relative amounts of magnetite (S-parameter values >0.85) in most samples from western and central parts of

the transect (Figure 4). The systematic and sharp increase in relative hematite contents (S-parameter values <0.85) as well as HIRM values (Figure 3) at all depths in the easternmost four sites reflect the position of the sampling

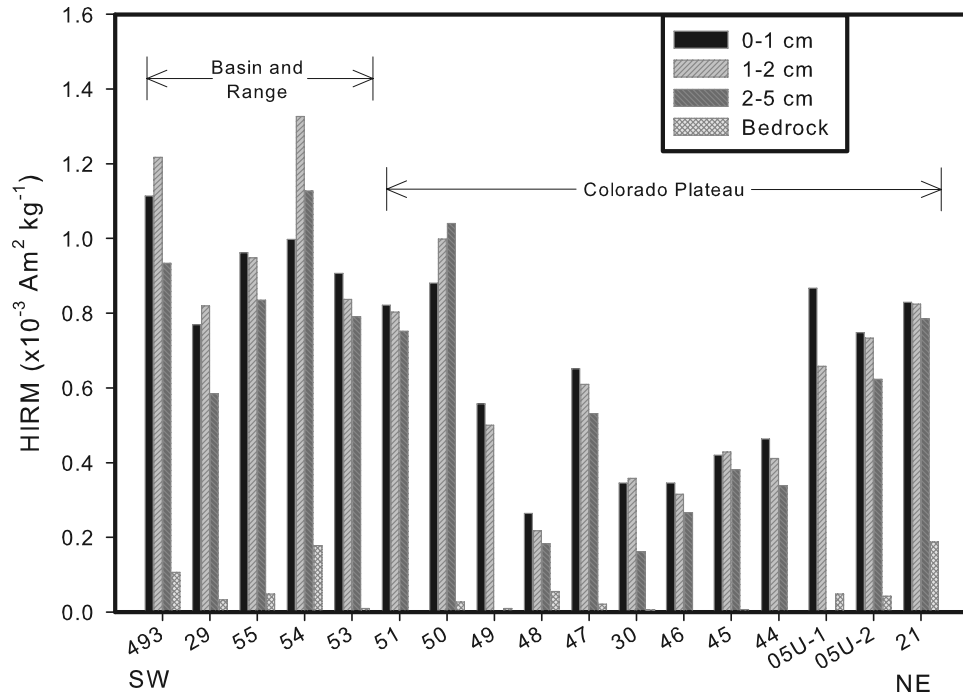


Figure 3. Bar plot of HIRM (hematite) for pothole sediment and bedrock. Hematite content is highest at the southwestern sites but is also elevated at sites located on the central Colorado Plateau. Hematite is much more abundant in the sediment samples than in the associated bedrock.

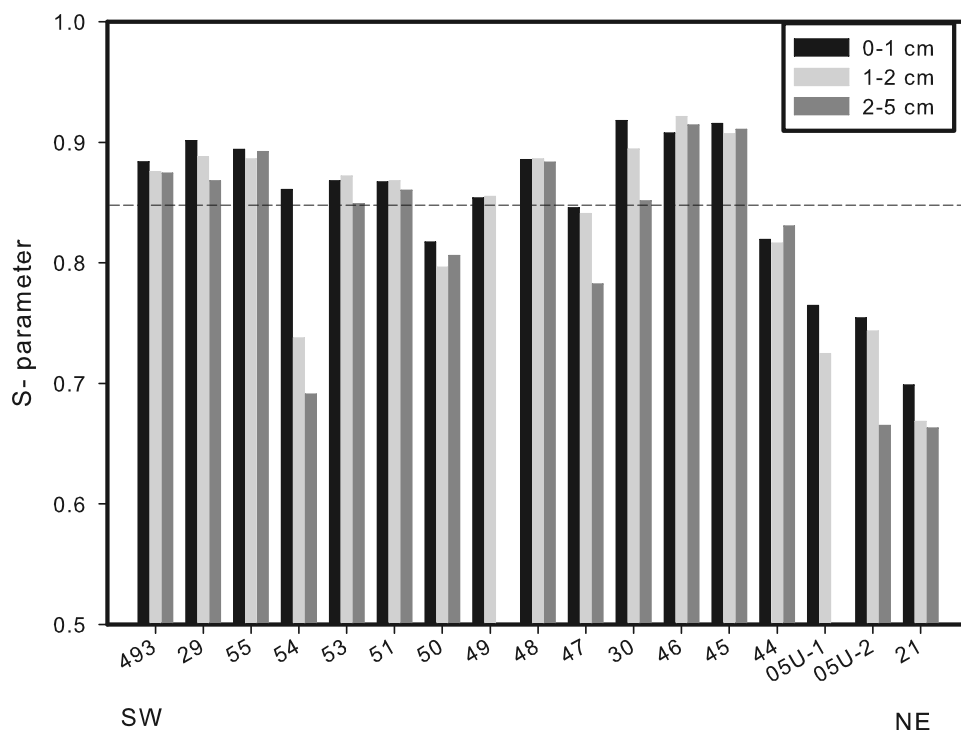


Figure 4. Bar plot of S-parameter, an indicator of relative amounts of magnetite and hematite for pothole sediment. Highest relative amounts of magnetite are in samples from the western and central portion of the transect. Higher relative amounts of hematite are in samples from the central Colorado Plateau. Dashed line represents the S-parameter value of 0.85. Values greater than 0.85 contain higher relative amounts of magnetite than values less than 0.85.

sites within the area that harbors abundant exposures of redbeds.

[17] The distributions of magnetite ($IRM_{0.3T}$), when viewed in the sediment depth profile at each site, reveal a pattern that bears on contributions from dust sources over time. Magnetite abundance is highest in the shallow sample (0–1 cm depth) at 15 of the 17 sites, indicating that magnetite inputs over the study region have been highest during the most recent time of dust accumulation (Figure 2). The distributions of hematite in site profiles do not show a similar pattern, although hematite is highest in the top sample at most sites on the Colorado Plateau (Figure 3).

4.2. Particle Size

[18] The pothole sediments are considerably finer textured than the bedrock in which they are deposited. Average sand, silt, and clay percentages of the pothole sediments are 72%, 18%, and 7%, respectively. The bedrock in which the potholes are formed has an average textural composition of 93% sand, 4% silt, and 3% clay with little variation between sites. The difference in fines (silt plus clay) between pothole sediment and sandstone gives a rough indication of the amount of aeolian dust in these sediments. The silt- and clay-size fractions ($<63 \mu\text{m}$) of most pothole-sediment samples exhibit elevated abundances of fines centered at about 10–20 μm (Figure 5). Most sediment samples from Colorado Plateau sites also contain abundant fines in size classes centered on about 6 μm and 2 μm . Thus, the pothole deposits from sites on the Colorado Plateau contain relatively more fine-grained sediment than sites located in the

Mojave Desert. All depths of sediment within each pothole are dominated by sand size particles (typically $>50\%$). Silt contents for all depths are typically 10–30%, and clay contents for all depths are typically less than 10%. There do not appear to be any consistent textural trends with sample depth within the potholes (data not shown; see Goldstein *et al.* [2007]).

4.3. Chemical Properties

[19] Pothole sediment and bedrock differ greatly in chemical composition. Pothole sediment is elevated relative to the bedrock in many common major and minor elements (e.g., Ti, Fe, Zr, Mn, Cu, Al, K, Mg, Na, P, Pb, Zn, Cd; Figure 6). Calcium is high in bedrock samples because they typically contain abundant calcite cement.

[20] Similar to magnetite, many elements in the surface sediment decrease in abundance to the northeast (e.g., Al, Fe, Cr, Mg, Na, Zn, Cu, and Pb; Figure 7). Zirconium is the only element that shows a distinct northeasterly increase in abundance along the transect (Figure 7). To evaluate the spatial distributions of elements that are potential plant nutrients, we summed the normalized values of the macronutrients and micronutrients K, Mg, P, Na, Fe, Mn, Zn, Cu, Mo, Ni, and Co [Marschner, 1995] for each sample. These normalized nutrient values also tend to decrease toward the northeast for pothole-sediment samples from all depths (Figure 8). Some chemical trends change with depth in the pothole sediment. Expressed as normalized averages (individual elements were averaged for each depth and bedrock at all sites and then normalized to the highest average) for all samples, some

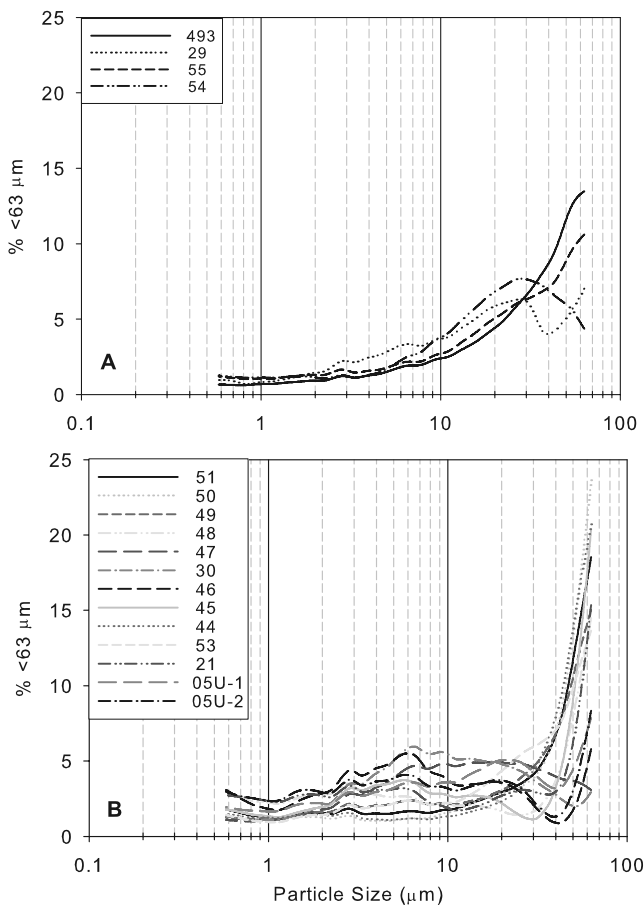


Figure 5. Particle size distributions of the pothole surface sediment (0–1 cm) fine fraction (silt + clay) on a log scale showing elevated abundance of fine grained material displayed as percent of the less than 63-micron size fraction ($\% < 63 \mu\text{m}$). (a) Sites located west of the Colorado Plateau. (b) Sites located on the Colorado Plateau.

elements decrease in abundance with depth (e.g., Mn, Mg, Na, P, Pb, Zn, and Cd; examples shown on Figure 6). Aluminum is the only element that increases with depth, and Fe and K are nearly constant with depth. Although Ti (depleted in the surface sample) and Zr do not have consistent depth trends, Zr/Ti decreases with depth (Figure 6).

4.4. Strontium Isotopes

[21] Distinctions between pothole sediment and bedrock can also be evaluated by comparing their isotopic compositions. Strontium isotopes of the leached (labile) and residual fractions has been used to examine atmospheric inputs to soils in arid lands in the American Southwest [e.g., Capo *et al.*, 1998; Capo and Chadwick, 1999; Van der Hoven and Quade, 2002]. Values of $^{87}\text{Sr}/^{86}\text{Sr}$ of the labile fraction of the pothole surface sediment fines range between 0.7082 and 0.7107 and are less radiogenic than that of the associated bedrock (0.7084–0.7122) (Figure 9). In general, the labile fraction of the sandstone bedrock across the transect (mean = 0.7106, SE = 0.00031, $n = 13$) is substantially more radiogenic than basalt located near site 45 (0.7084) or limestone from site 51 (0.7072). The broad differences between sandstones and other bedrock sub-

strates is even more pronounced for the residual fraction where sandstones are highly radiogenic (mean = 0.7244, SE = 0.00176, $n = 13$) compared to the basalt (0.7054) or limestone (0.7078). The large difference between the labile and residual Sr isotopic content of sandstones arises from the mineralogy of these rocks that is dominated by silica minerals cemented by carbonates, which are relatively easily leached. Such a large difference is not evident in lithologies that do not contain high concentrations of easily soluble carbonates, such as igneous rocks or carbonate rocks.

5. Discussion

5.1. Recognition of Aeolian Dust

[22] Magnetic, petrographic, isotopic, chemical, and textural data indicate the presence and accumulation of aeolian dust that mixed with locally derived sediment in the potholes. These sediments contain abundant detrital, silt-sized magnetite and related Fe-Ti oxide minerals, all of which are lacking in local bedrock. At all of the study sites hematite is strongly enriched in the sediments relative to local bedrock, despite the presence of hematite in bedrock at some sites (Table 1). The magnetic properties, complemented by petrographic observations, indicate the presence of a substantial amount of atmospheric dust in pothole sediment. The amount of fines in the bulk sediment (average volume, 25%) compared with that in associated sandstone (less than 10%) suggests that the dust component is in the range of 15–20% by volume. This amount is similar to estimates made on pothole-fill sediment elsewhere on the central Colorado Plateau [Reynolds *et al.*, 2001a, 2006a]. In the sediment samples of this study, the abundance of particles in the 2–12 μm size classes indicates a substantial component of far-traveled dust [Goudie and Middleton, 2006], perhaps on the order of many tens to hundreds of kilometers.

[23] Chemical data indicate contrasting mineral compositions and thus further reveal an external source for some of the pothole sediment. Most analyzed elements show higher abundance in the pothole fines ($< 63 \mu\text{m}$) compared to the associated bedrock, indicating that the pothole sediment fine fraction did not originate solely from the weathering of the associated bedrock (Figure 6). Comparison of major element chemistry illustrates the differences in chemical composition between sediment and bedrock. Discriminant analysis performed using weighted major element chemistry [see Rollinson, 1998] shows the pothole sediment samples are shifted toward the felsic igneous province away from the quartzose sedimentary province occupied by most bedrock samples from this study (Figure 10) [Rollinson, 1998]. This shift represents sediment accumulation from sources that have more felsic compositions than the local sedimentary rocks in which the potholes are formed.

[24] Additional mineralogic differences between sediment and bedrock are seen in $^{87}\text{Sr}/^{86}\text{Sr}$ values of the labile minerals. Carbonate minerals in the fine fraction of the pothole sediment are less radiogenic than those in the associated bedrock (Figure 9). These results are consistent with a component of a non-local mineral source for the pothole fines because if the pothole fines were derived from the associated bedrock as weathered detritus, they would yield comparable radiogenic values to the sandstone bedrock.

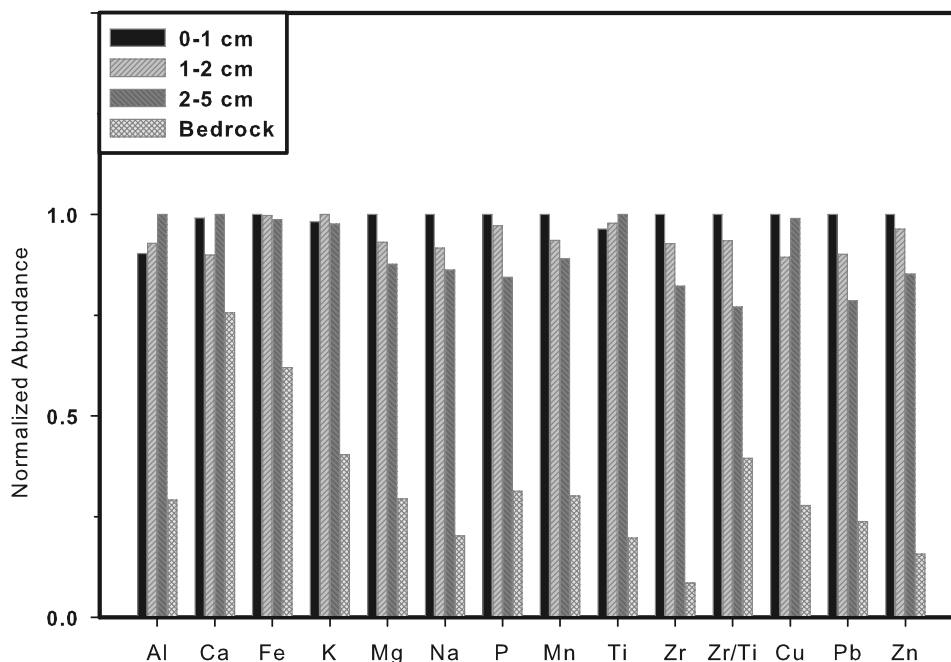


Figure 6. Bar plot showing averaged, normalized chemical compositions of pothole sediment ($n = 16$) by depth and bedrock ($n = 15$ except Ca where $n = 14$). Site 46 sediment and bedrock was omitted because of lack of sample for chemical analyses. Site 51 bedrock was omitted from Ca because it is limestone. Chemical compositions were normalized for each depth to the highest averaged value.

5.2. Spatial Trends in Aeolian Sediment

[25] Many other studies have examined atmospheric dust in soil and surficial deposits because of the importance of dust to landscape and ecosystem dynamics. A large and growing body of literature exists on this topic applied to drylands [e.g., *Yaalon and Ganor, 1973; Wells et al., 1985, 1987; McFadden et al., 1986, 1987, 1998; Chadwick and Davis, 1990; McDonald et al., 1996; Belnap and Gillette, 1998; Shachak and Lovett, 1998; Reynolds et al., 2001a*]. Our investigation of a large region spanning several desert ecosystems in the southwestern United States reveals the influences of many dust sources, including a major dust source region along with many local ones, on the compositions of deposited dust in this region.

[26] The general southwest-to-northeast decrease in magnetite content (indicated by the overall decrease in $IRM_{0.3T}$ values) of the pothole sediment fines (Figure 2) can be attributed to at least two factors. First, this pattern may reflect aerodynamic sorting from magnetite-bearing dust sources in the western part of the transect. Magnetite-bearing rocks are common in the Mojave Desert [*North American Magnetic Anomaly Group, 2002*]. Sediments derived from them are well mixed in dust source areas, and dust sequestered within the surface soils and sediments of the Mojave Desert contains abundant magnetite [*Reynolds et al., 2006c*]. Second, the decline in magnetite content may reflect the regional distribution of magnetite-bearing rock across the sampled region. As previously stated, old sedimentary rocks, the most widely exposed lithic types on the Colorado Plateau, contain little or no magnetite, and magnetite-bearing igneous rocks are sparse on the Plateau with the exception of basaltic to rhyolitic volcanic fields mostly at the margins (Figure 1).

[27] Similar to magnetite content, hematite content generally decreases in abundance northeasterly along the transect (Figure 3). However, hematite content increases at sites located on the central Colorado Plateau, in the vicinity of Canyonlands National Park, Utah. This abrupt increase in hematite content is likely due to the contribution of dust from hematite-rich sedimentary rocks, which are widespread on this part of the Colorado Plateau [*Huntoon et al., 1982*]. Contributions of hematite-rich dust in this area are further supported by S-parameter values (Figure 4), with the low values indicating relatively high proportions of hematite.

[28] Strontium isotopic data also show variation across the region. Considering the spatial variation of Sr isotope values of labile and residual fractions of different bedrock types along our transect, and the multitude of potential dust sources (and isotopic signals), it is difficult to use absolute Sr isotope measurements to link the spatial variability to potential dust source areas. However, the ratio of the Sr isotopic ratio of the labile and residual fractions (Sr L/R) expressed as $100 * ({}^{87}\text{Sr}/{}^{86}\text{Sr}_{\text{Residual}} - {}^{87}\text{Sr}/{}^{86}\text{Sr}_{\text{Labile}}) / ({}^{87}\text{Sr}/{}^{86}\text{Sr}_{\text{Residual}})$ provides a qualitative indication of the potential source materials for pothole sediment. High values of this ratio indicate large differences between residual and labile Sr isotopic contents, which may characterize calcite-cemented sandstones, whereas lower values (near unity) appear to reflect other bedrock sources of sediment. The ratio of labile to residual Sr in both the sand and fine fractions of the pothole sediment shows wide variation across the transect. In general, both fractions show much lower values for the sites closest to the Mojave Desert and higher values in the northeastern sites on the Colorado Plateau (Figure 11). In comparison, the Sr L/R ratio for

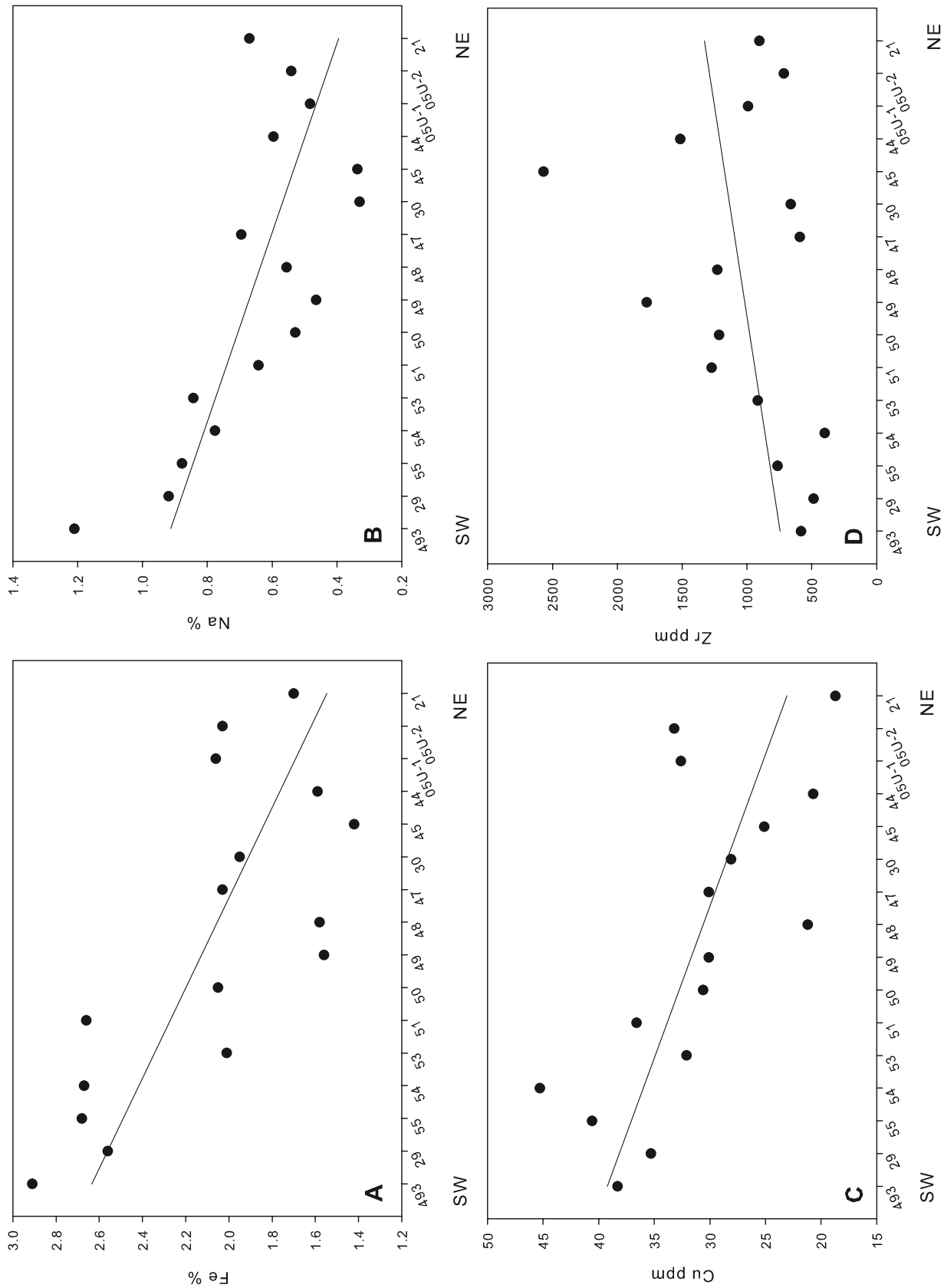


Figure 7. Scatterplots of pothole surface sediment (0–1 cm) showing the northeasterly decrease in selected elements, Fe, Na, Cu, Zr (A – C), and the northeasterly increase in Zr (D).

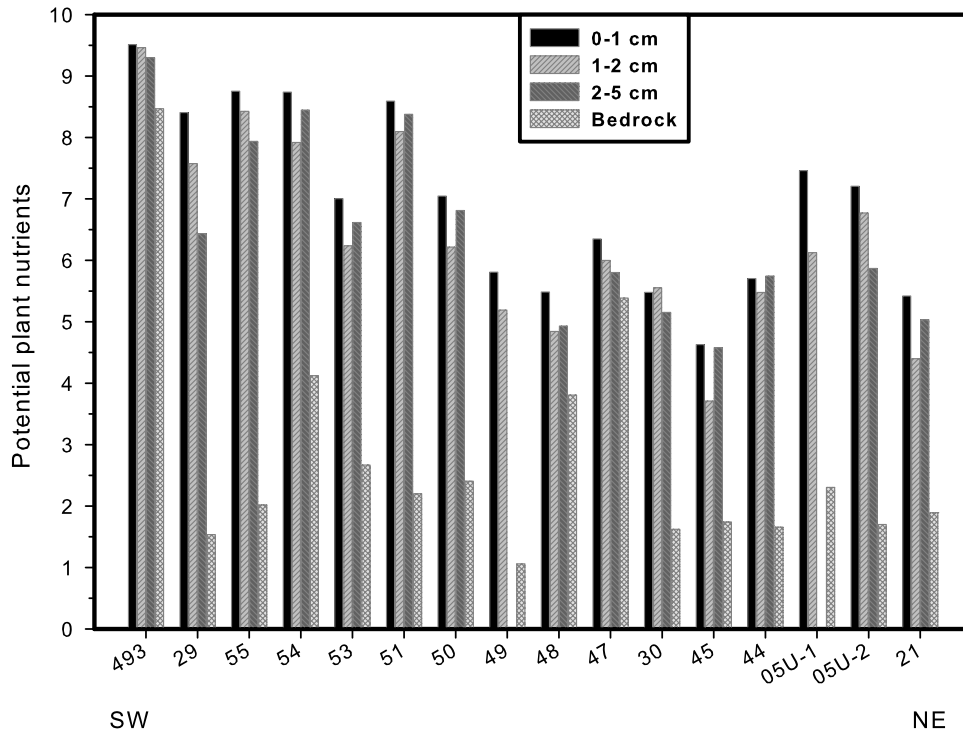


Figure 8. Bar plot showing potential plant nutrients for pothole sediment and bedrock. Potential plant nutrients generally decrease to the northeast. Potential plant nutrient values are reported here as the sum of the normalized nutrient concentrations. Nutrients were normalized to the highest averaged abundance as in Figure 6.

the basalt sample near site 45 is -0.43, for the limestone (at site 51) is 0.08, and for the sandstones (at site 51) is 1.95 (SE = 0.24). Overall, the relatively low Sr L/R ratios in the fine fraction of sediments provide additional support for the input of far-traveled, nonlocal sediments to the Colorado Plateau sites.

Although preliminary, the use of Sr L/R ratios might offer the potential for further distinctions among sources of dust to soil across the Southwestern United States as more information on the Sr isotopic content of bedrock in the region becomes available.

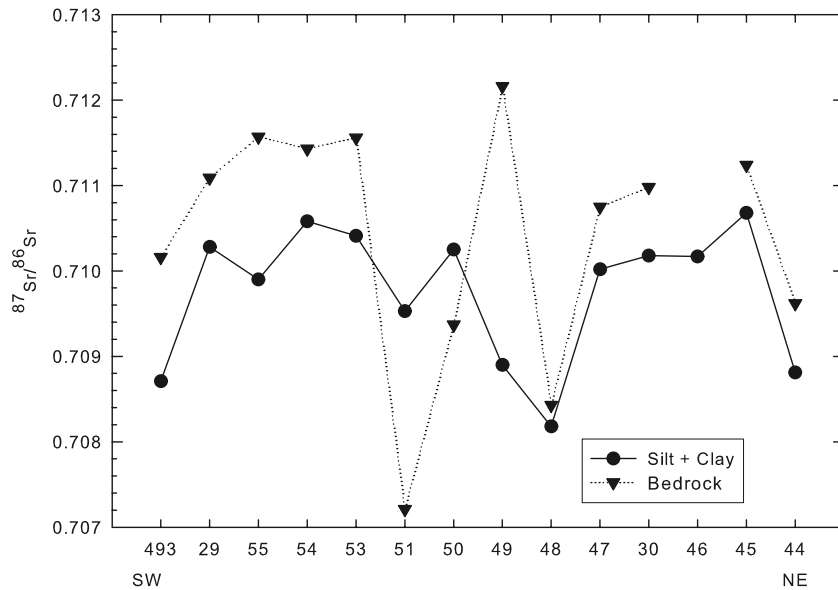


Figure 9. $^{87}\text{Sr}/^{86}\text{Sr}$ values of the acid-soluble carbonate minerals (labile fraction) in the pothole fine fraction (0–1 cm) and associated bedrock. Carbonates in the pothole sediment are less radiogenic than the associated bedrock, indicating that the fine fraction of the pothole sediment did not originate by weathering of the associated bedrock. Easternmost sample sites were not analyzed.

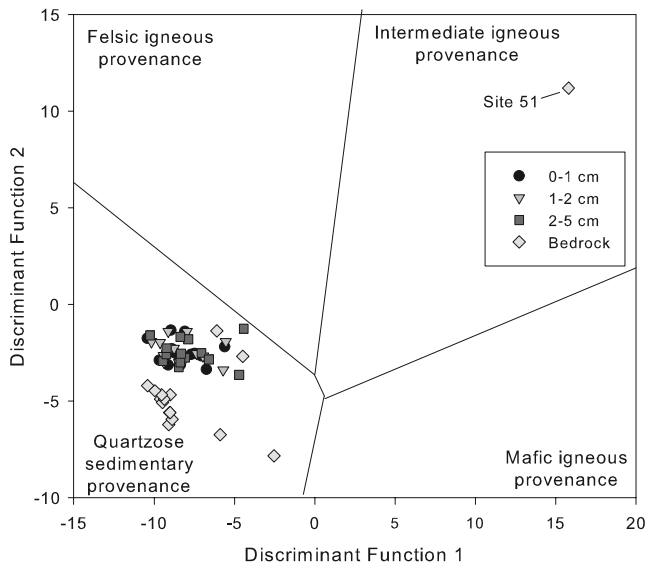


Figure 10. Discriminant diagram of pothole sediment and bedrock (adapted from *Rollinson [1998]*). Diagram shows that pothole sediments shift toward the felsic igneous province away from the quartzose sedimentary province occupied by most bedrock samples. Three bedrock samples are outliers due to high amounts of calcium.

[29] Spatial differences also exist with respect to pothole-sediment texture. Although all sites contain abundances in the size classes that are characteristic of far-traveled dust, pothole sediments at sites located on the Colorado Plateau are finer textured than sites located west of the Colorado Plateau (Figure 5). The finer pothole sediment texture and

the general decreases in magnetite and hematite content along the transect provide the strongest evidence for aerodynamic sorting of dust derived from the west as it was transported across the study area, with depletion of relatively coarse particles and relatively high-density minerals toward the northeast. However, similar evidence for sorting is not evident from the chemical data. It would be expected, for example, that Ti abundance would show a similar pattern to that of magnetite content (decreasing to the northeast) because of the association of Ti with magnetite and related minerals, and this is not the case (Figure 12). Zirconium is another chemically stable element that might be expected to show effects of aerodynamic sorting [see *Mason and Jacobs, 1998; Muhs and Bettis, 2000*] but does not (Figure 12). Overall, Zr abundance varies greatly spatially and with depth at most sites, even though Zr content of bedrock is uniformly low, as expected. These strong variations in Zr are difficult to explain.

[30] The amounts of potential nutrients generally decrease along the transect (Figure 8), similar to the trends in hematite and magnetite. One way to evaluate the importance of dust from different sources (sources associated with magnetite compared with those that lack magnetite) is to compare $IRM_{0.3T}$ (magnetite) and HIRM (hematite) with potential plant nutrients (Figure 13). The comparisons between the concentrations of magnetite and hematite and potential nutrients (Figure 13) suggest that these components are generally linked by common source areas, despite the known complexity about the locations and timing of dust sources in the southwestern United States [e.g., *Brazel and Nickling, 1987; Bach et al., 1996; Reheis, 2006*].

[31] In the uppermost samples, metals that may be associated with airborne pollutants decrease in abundance

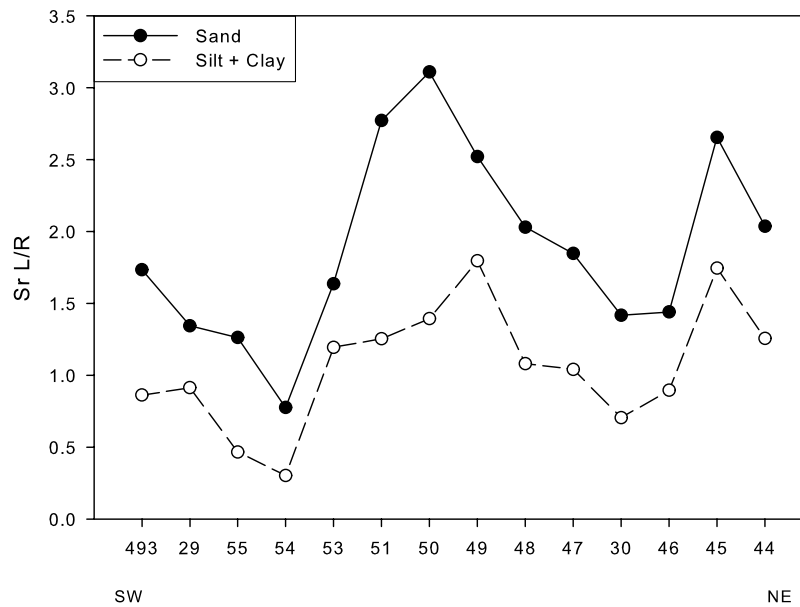


Figure 11. Strontium labile/residual ratio (Sr L/R) of pothole sediment (0–1 cm) sand and fine (silt+clay) fractions. Sr L/R for both size fractions are generally lowest at the southwestern sites and are higher at the northeastern sites. The lower Sr L/R values for fine fraction (mean = 1.08) and the elevated Sr L/R values for the sand fraction (mean = 1.94) are consistent with nonlocal and local sources, respectively.

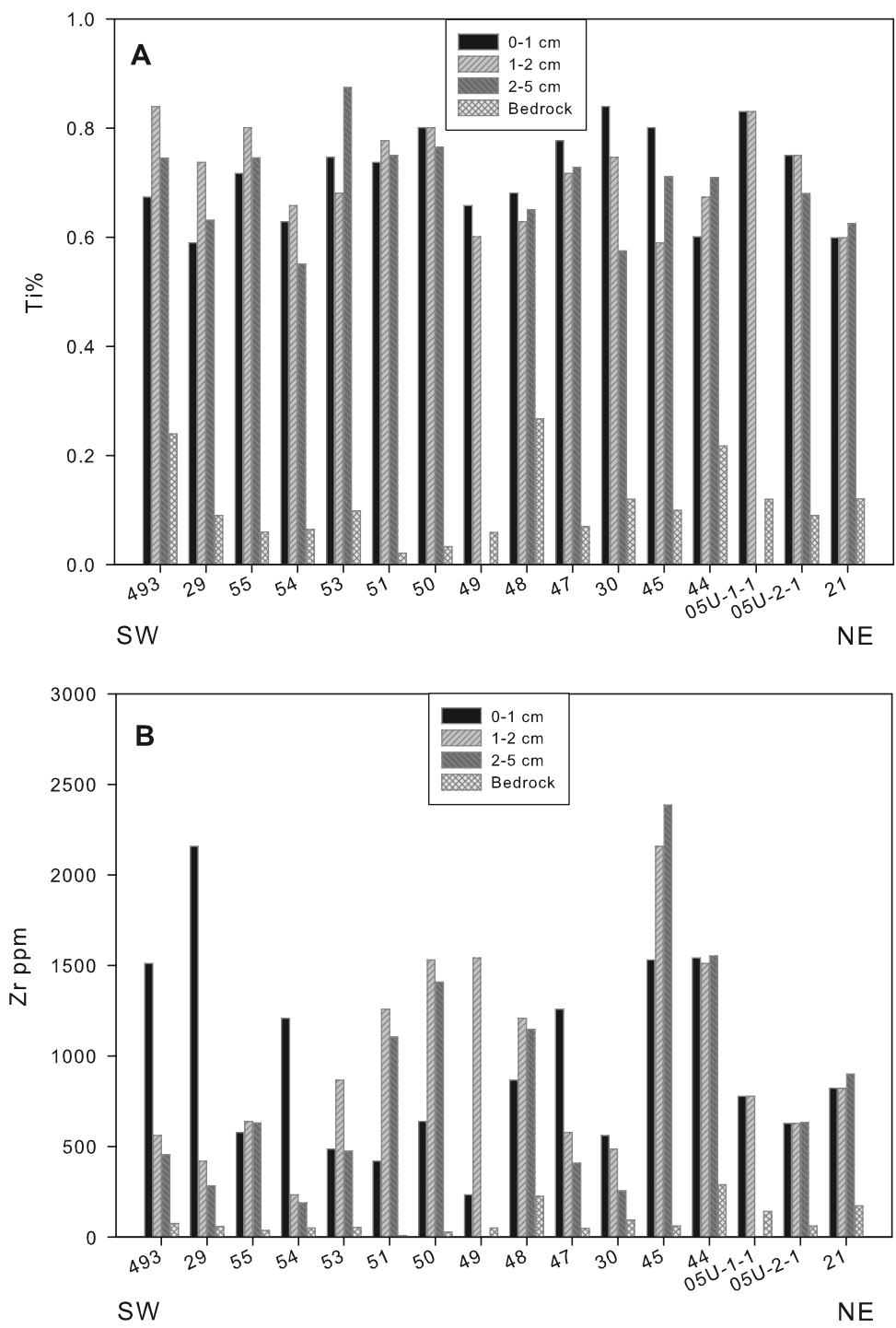


Figure 12. Bar plots of (a) titanium and (b) zirconium values for pothole sediment and associated bedrock. Neither plot suggests aerodynamic sorting. Titanium usually associated with Ti-bearing magnetic material (magnetite) does not follow the same spatial pattern as magnetite (decrease to northeast). Zirconium is highly variable both spatially and with depth.

to the northeast. The relatively high abundance of these metals (e.g., Zn, Cu, and Pb) in the southwesternmost sites may be related to anthropogenic activity considering their locations near the city of Las Vegas, Nevada, and in the path of smog plumes from highly populated areas of southern California [Lyons *et al.*, 1999] (Figure 14). Work

is continuing to assess possible anthropogenic signatures contained within dust.

5.3. Temporal Trends in Aeolian Sediment

[32] Systematic differences in physical and chemical properties between 0-1 cm sediment and underlying sedi-

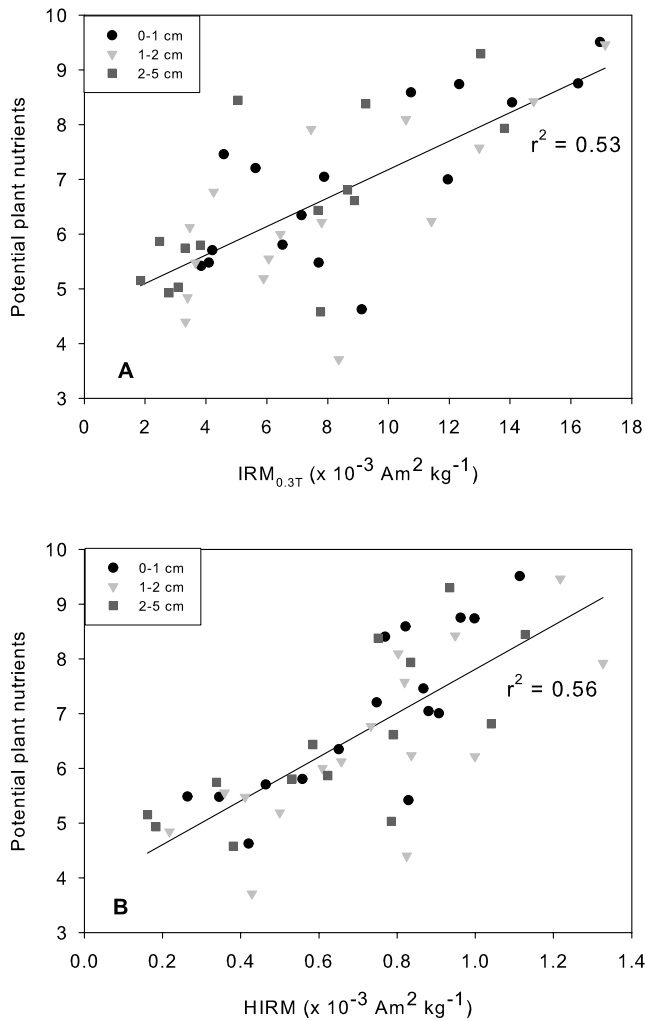


Figure 13. Comparisons between potential plant nutrients and (a) magnetite and (b) hematite, showing similar correlations for all pothole sediment depths. Potential plant nutrients displayed as in Figure 8.

ment probably record changes in some aspects of dust inputs, whether in amounts of dust emission from common sources or the advent of new sources. In these thin pothole sediments, there is no petrographic or chemical evidence for pedogenic alteration of magnetic minerals or for leaching of relatively soluble components documented for older, deeper desert soils [see *McFadden et al.*, 1998; *Reynolds et al.*, 2006c]. In general, the pattern of decrease in magnetite abundance toward the northeast is seen at all sample depths (Figure 2). This pattern perhaps suggests that the regional distribution of dust fall and thus the locations of principal sources have not changed greatly over the period represented by our sampling. Relative to the top layer, magnetite abundance at depth shows more variability with more abrupt changes (e.g., sites west of site 50). The pattern of magnetite distribution may thus reflect relatively more contribution from dominant Mojave Desert sources during the past century (depths below 1 cm).

[33] Magnetite abundance is highest in the top sample for 15 of 17 sites, suggesting higher magnetite flux during the

past several decades than prior centuries. This pattern is not seen in Fe or Ti contents (Figure 12), but this lack of correspondence is not surprising considering that magnetite concentrations (less than 0.5%) make up a very small proportion of the Fe and Ti loads.

[34] Amounts of potential nutrients also change over time. Highest values are found in the top sample at 15 of 17 sites (Figure 8), suggesting recent increases in the amounts of nutrients delivered by dust. We lack chronologic control on the timing of such recent increases, but they correspond spatially with the presence of biologic soil crust. On this basis, we surmise increased delivery of dust during the past several decades to about a century, as similarly concluded by *Reynolds et al.* [2001a] for similar settings. A similar conclusion was found for a set of pothole sites in the Canyonlands area of the Colorado Plateau [*Reynolds et al.*, 2001a], implying that this observation may be extended across the region.

6. Conclusions

[35] The primary goal of this study was to evaluate the spatial and temporal variations and trends in physical and chemical properties of dust along a transect from the Mojave Desert to the central Colorado Plateau. Composition and texture of fine-grained sediment in potholes on isolated surfaces on the Colorado Plateau suggest far-distant sources, at least some from beyond the Colorado Plateau, as well as local sources. Magnetic minerals can be used as crude tracers for dust source areas. Many types of igneous bedrock units in the Mojave Desert contain appreciable amounts of magnetite, but vast areas of the Colorado Plateau are underlain by hematite-rich sedimentary rocks that lack magnetite. With these observations on regional distributions of Fe-oxide minerals as guides, the spatial and temporal distributions of magnetite and hematite in the pothole sediment suggest relatively more contributions to Colorado Plateau landscapes from the Mojave Desert during the past century.

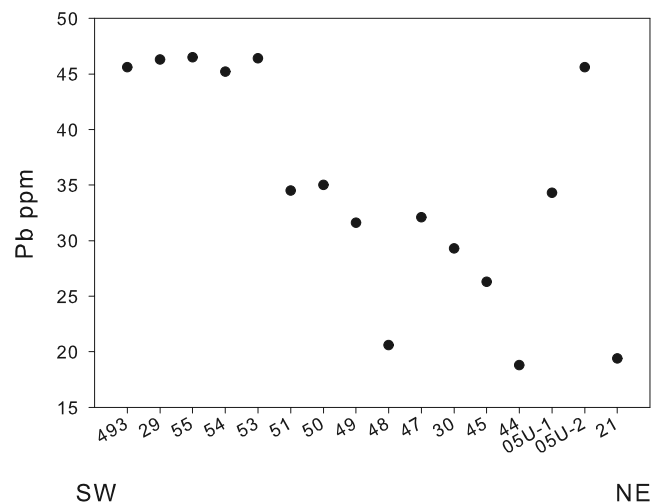


Figure 14. Lead contents in pothole surface sediment (0–1 cm) showing elevated amounts in the southwestern sites that may be related to anthropogenic activity.

[36] Soil development in drylands is controlled by many factors, among them additions of wind-blown sediment. This study documents additions of potential nutrients from dust onto landscapes characterized by old, nutrient-poor sedimentary rocks. In the study region, some potential nutrients vary in relation to the inferred influence of the Mojave Desert as a major dust source. Moreover, the addition of potential nutrients has varied over the short-time interval represented by our samples, on the order of a few centuries. The most consistent change appears to be small enhancement of potential nutrients during the past century (represented by samples from 0 to 1 cm depth). The increase in nutrient inputs corresponds to increases in magnetite deposition; together they suggest enhanced dust emission in the American Southwest from magnetite-bearing sources such as the Mojave Desert. On the basis of regional geology, contributions from other areas are likely. Human disturbances of deserts in the southwestern United States that act as dust sources may be a factor in producing changes in the composition of far-traveled dust and thus can play an important role toward soil geochemistry in far-distant areas on the Colorado Plateau.

[37] **Acknowledgments.** We thank Yarrow Axford for assistance in sample collection and laboratory analysis; Eric Fisher, Jiang Xiao, Ken Takagi, and Isla Casteñeda for laboratory analyses; Kathleen Simmons for Sr isotope analysis; and Paul Lamothe for chemical analysis. This manuscript benefited from reviews by Corey Lawrence, Lesleigh Anderson, Mark Sweeney, and one anonymous reviewer. This work was supported by the Earth Surface Dynamics Program of the United States Geological Survey.

References

- Bach, A. J., A. J. Brazel, and N. Lancaster (1996), Temporal and spatial aspects of blowing dust in the Mojave and Colorado Deserts of southern California, *Phys. Geogr.*, *17*, 329–353.
- Belnap, J. (1993), Recovery rates of cryptobiotic crusts: Inoculate use and assessment methods, *Great Basin Natural.*, *53*, 89–95.
- Belnap, J., and D. A. Gillette (1998), Vulnerability of desert biological soil crusts to wind erosion: the influences of crust development, soil texture, and disturbance, *J. Arid Environ.*, *39*, 133–142.
- Bohannon, R. G. (1978), Geologic map of the Las Vegas 1° × 2° quadrangle, Nevada, Arizona, and California, *U.S. Geol. Surv. Open File Rep.*, *78-670*, 1:250,000.
- Brazel, A. J., and W. G. Nickling (1987), Dust storms and their relation to moisture in the Sonoran-Mojave Desert region of the south-western United States, *J. Environ. Manage.*, *24*, 279–291.
- Capo, R. C., and O. A. Chadwick (1999), Sources of strontium and calcium in desert soil and calcrete, *Earth Planet. Sci. Lett.*, *170*, 61–72.
- Capo, R. C., B. W. Stewart, and O. A. Chadwick (1998), Strontium isotopes as tracers of ecosystem processes: Theory and methods, *Geoderma*, *82*, 197–225.
- Chadwick, O. A., and J. O. Davis (1990), Soil-forming intervals caused by eolian sediment pulses in the Lahontan basin, northwestern Nevada, *Geology*, *18*(3), 243–246.
- Chadwick, O. A., L. A. Derry, P. M. Vitousek, D. A. Huebert, and L. O. Hedin (1999), Changing sources of nutrients during four million years of ecosystem development, *Nature*, *397*, 491–497.
- Chavez, P. S., Jr., D. J. MacKinnon, R. L. Reynolds, and M. Velasco (2002), Monitoring dust storms and mapping landscape vulnerability to wind erosion using satellite and ground-based digital images, *Arid Lands NewsL.*, *51*. (Available at <http://ag.arizona.edu/OALS/ALN/aln51/chavez.html>)
- Eppinger, R. G., G. R. Winkler, T. M. Cokro, M. A. Shubat, H. R. Blank, J. K. Crowley, R. P. Kucks, and J. L. Jones (1990), Preliminary assessment of the mineral resources of the Cedar City 1° × 2° quadrangle, Utah, *U.S. Geol. Surv. Open File Rep.*, *90-34*, 1:250,000.
- Evans, M. E., and F. Heller (2003), *Environmental Magnetism*, 299 pp., Academic, Amsterdam.
- Gill, T. E. (1996), Eolian sediments generated by anthropogenic disturbance of playas: Human impacts on the geomorphic system and geomorphic impacts on the human system, *Geomorphology*, *17*, 207–228.
- Goldstein, H. L., R. L. Reynolds, M. C. Reheis, J. C. Yount, and P. J. Lamothe (2007), Physical and chemical data from eolian sediment collected along a transect from the Mojave Desert to the Colorado Plateau, *U.S. Geol. Surv. Open File Rep.* *2007-1153*, 29 pp.
- Goudie, A. S., and N. J. Middleton, (2006), *Desert Dust in the Global System*, 287 pp., Springer, Amsterdam.
- Graf, W. L., R. Hereford, J. Laity, and R. A. Young (1987), Colorado Plateau, in *Geomorphic Systems of North America: Boulder, Colorado*, vol. 2, edited by W. L. Graf, pp. 259–302, Geol. Soc. of Am., Reston, Va.
- Hackman, R. J., and D. G. Wyant (1973), Geology, structure, and Uranium deposits of the Escalante quadrangle, Utah and Arizona, *U.S. Geol. Surv. Misc. Geol. Invest.*, *Map I-744*, 1:250,000.
- Haggerty, S. E. (1976), Opaque mineral oxides in terrestrial igneous rocks, in *Oxide Minerals, Short Course Not.*, vol. 3, edited by D. Rumble, pp. Hg101–Hg300, Mineral. Soc. of Am., Chantilly, Va.
- Haynes, D. D., J. D. Vogel, and D. G. Wyant (1972), Geology, structure, and Uranium deposits of the Cortez quadrangle, Colorado and Utah, *U.S. Geol. Surv. Misc. Geol. Invest.*, *Map I-629*, 1:250,000.
- Hunt, C. B. (1956), Cenozoic geology of the Colorado Plateau, *U.S. Geol. Surv. Prof. Pap.*, *279*, 99 pp.
- Huntoon, P. W., G. H. Billingsley, and W. J. Breed (1982), Geologic map of Canyonlands National Park and vicinity, Utah, Canyonlands Natl. History Assoc., Moab, Utah.
- Jennings, C. W. (1961), Geologic map of California, Kingman sheet, Dept. of Natural Resour., Calif. Div. of Mines and Geol., Sacramento.
- King, P. B., and H. M. Beikman (1974), Geologic map of the United States, 1:2,500,000, *U.S. Geol. Surv.*, Reston, Va.
- Lauf, R. J. (1982), Microstructures of coal fly ash particles, *Ceramic Bull.*, *61*, 487–490.
- Lauf, R. J., L. A. Harris, and S. S. Rawlson (1982), Pyrite framboids as the source of magnetite spheres in fly ash, *Environ. Sci. Technol.*, *16*, 218–220.
- Lichte, F. E., D. W. Golightly, and P. J. Lamothe (1987), Inductively coupled plasma-atomic emission spectrometry, in *Methods for Geochemical Analysis*, edited by P. A. Baedeker, *U.S. Geol. Surv. Bull.*, *1770*, p. B1–B10.
- Lipman, P. W. (2000), Central San Juan caldera cluster: Regional volcanic framework, *Geol. Soc. Am. Spec. Pap.*, *346*, 9–69.
- Luedke, R. G., and R. L. Smith (1978), Map showing distribution, composition, and age of late Cenozoic volcanic centers in Arizona and New Mexico, *U.S. Geol. Surv. Misc. Invest. Ser.*, *Map I-1091-A*, scale 1:100,000 and 1:500,000, 2 sheets.
- Lyons, J. M., C. Venkataraman, H. H. Main, and S. K. Friedlander (1999), Size distributions of trace metals in the Los Angeles atmosphere, *Atmos. Environ., Part B*, *27*(2), 237–249.
- Machette, M. (1986), Calcium and magnesium carbonates, in *Field and Laboratory Procedures Used in a Soil Chronosequence Study*, edited by M. Singer and P. Janitzky, *U.S. Geol. Surv. Bull.* *1648*, 30–33.
- Marschner, H. (1995), *Mineral Nutrition of Higher Plants*, 2nd ed., 889 pp., Academic, London.
- Mason, J. A., and P. M. Jacobs (1998), Chemical and particle-size evidence for addition of fine dust to soils of the midwestern United States, *Geology*, *26*, 1135–1138.
- McDonald, E. V., L. D. McFadden, and S. G. Wells (1995), The relative influences of climate change, desert dust, and lithologic control on soil-geomorphic processes on alluvial fans, Mojave Desert, California: Summary of results, in *Ancient Surfaces of the East Mojave Desert*, edited by R. E. Reynolds and J. Reynolds, *San Bernardino County Museum Assoc. Quart.*, *42*, 35–42.
- McDonald, E. V., F. B. Pierson, G. N. Flerchinger, and L. N. McFadden (1996), Application of a process-based soil-water balance model to evaluate the influence of Late Quaternary climate change on soil-water movement in calcic soils, *Geoderma*, *74*, 167–192.
- McFadden, L. D., S. G. Wells, and J. C. Dohrenwend (1986), Influences of Quaternary climatic changes on processes of soil development on desert loess deposits of the Cima volcanic field, California, *Catena*, *13*, 361–389.
- McFadden, L. D., S. G. Wells, and M. J. Jercinovich (1987), Influences of eolian and pedogenic processes on the origin and evolution of desert pavements, *Geology*, *15*, 504–508.
- McFadden, L. D., E. V. McDonald, S. G. Wells, K. Anderson, J. Quade, and S. L. Forman (1998), The vesicular layer and carbonate collars of desert soils and pavements: formation, age, and relation to climate change, *Geomorphology*, *24*, 101–145.
- Muhs, D. R. (1983), Airborne dust fall on the California Channel Islands USA, *J. Arid Environ.*, *6*, 223–238.
- Muhs, D. R., and J. B. Benedict (2006), Eolian additions to late Quaternary alpine soils, Indian Peaks Wilderness Area, Colorado Front Range, *Arctic Antarct. Alpine Res.*, *38*(1), 120–130.

- Muhs, D. R., and E. A. Bettis (2000), Geochemical Variations in Peoria loess of western Iowa indicate paleowinds of midcontinental North American during last glaciation, *Quat. Res.*, *53*, 49–61.
- North American Magnetic Anomaly Group (2002), Magnetic Anomaly Map of North America, Special Map, *U.S. Geol. Surv.*, Reston, Va.
- Neff, J. C., R. L. Reynolds, J. Belnap, and P. Lamothe (2005), Multi-decadal impacts of grazing on soil physical and biogeochemical properties in southeast Utah, *Ecol. Appl.*, *15*(1), 87–95.
- Neff, J. C., R. L. Reynolds, R. L. Sanford, D. P. Fernandez, and P. Lamothe (2006), Geologic controls over soil and plant chemistry in southeastern Utah, *Ecosystems*, *9*, 879–893, doi:10.1007/s10021-005-0092-8.
- Nelson, S. T., and J. P. Davidson (1998), The petrogenesis of the Colorado Plateau laccoliths and their relationship to regional magmatism, in *Laccolithic Complexes of Southeastern Utah: Time of Emplacement and Tectonic Setting—Workshop Proceedings*, edited by J. D. Friedman and A. C. Huffman, *U.S. Geol. Surv. Bull.*, *2158*, 85–100.
- Page, W. R., et al. (2005), Geologic and geophysical maps of the Las Vegas 30' x 60' quadrangle, Clark and Nye counties Nevada and Inyo county, California, *U.S. Geol. Surv. Sci. Invest. Map*, *2814*, 1:100000.
- Patton, P. C., N. Biggar, C. D. Condit, M. L. Gillam, D. W. Love, M. N. Machette, L. Mayer, R. B. Morrison, and J. N. Rosholt (1991), Quaternary geology of the Colorado Plateau, in *Quaternary Nonglacial Geology: Conterminous U.S.: Boulder, Colorado*, edited by R. B. Morrison, *Geol. of N. Am.*, vol. K-2, pp. 373–406, Geol. Soc. of Am., Boulder, Colo.
- Pye, K. (1984), Loess, *Progr. Phys. Geogr.*, *8*(2), 176–217.
- Reheis, M. C. (2006), A 16-year record of eolian dust in southern Nevada and California, USA: Controls on dust generation and accumulation, *J. Arid Environ.*, *67*, 487–520.
- Reheis, M. C., and R. Kihl (1995), Dust deposition in southern Nevada and California, 1984–1989: Relations to climate, source area, and source lithology, *J. Geophys. Res.*, *100*(D5), 8893–8918.
- Reheis, M. C., J. R. Budahn, and P. J. Lamothe (2002), Geochemical evidence for diversity of dust sources in the southwestern United States, *Geochim. Cosmochim. Acta*, *66*, 1569–1587.
- Reheis, M. C., R. L. Reynolds, H. Goldstein, H. M. Roberts, J. C. Yount, Y. Axford, L. S. Cummings, and N. Shearin (2005), Late Quaternary eolian and alluvial response to paleoclimate, Canyonlands, southeastern Utah, *Geol. Soc. Am. Bull.*, *117*, 1051–1069.
- Reynolds, R. L., J. Belnap, M. Reheis, P. Lamothe, and F. Luiszer (2001a), Eolian dust in Colorado Plateau soils: Nutrient inputs and recent change in source, *Proc. Natl. Acad. Sci.*, *98*, 7123–7127.
- Reynolds, R. L., D. S. Sweetkind, and Y. Axford (2001b), An inexpensive magnetic mineral separator for fine-grained sediment, *U.S. Geol. Surv. Open File Rep.* *01-281*, *7*.
- Reynolds, R., et al. (2003), Dust emission and deposition in southwestern United States - integrated field, remote sensing, and modeling studies to evaluate response to climatic variability and land use, in *Desertification in the Third Millennium*, edited by A. S. Alsharhan et al., pp. 271–282, A. A. Balkema, Brookfield, Vt.
- Reynolds, R. L., J. C. Neff, M. C. Reheis, and P. Lamothe (2006a), Atmospheric dust in modern soil on aeolian sandstone, central Colorado Plateau Utah: Variation with landscape position and contribution to potential plant nutrients, *Geoderma*, *130*, 108–123.
- Reynolds, R. L., M. C. Reheis, J. C. Neff, H. Goldstein, and J. C. Yount (2006b), Late Quaternary eolian dust in surficial deposits of a Colorado Plateau grassland: Controls on distribution and ecologic effects, *Catena*, *66*, 251–266.
- Reynolds, R. L., M. C. Reheis, J. Yount, and P. Lamothe (2006c), Composition of aeolian dust in natural traps on isolated surfaces of the central Mojave Desert (USA)—insights to mixing, sources, and nutrient inputs, *J. Arid Environ.*, *66*, 42–61.
- Rollinson, H. (1998), *Using Geochemical Data: Evaluation, Presentation, Interpretation*, pp. 206–212, Longman Singapore, Jurong, Singapore.
- Rowley, P. D., C. C. Cunningham, T. A. Steven, H. H. Mehnert, and C. W. Naeser (1998), Cenozoic igneous and tectonic setting of the Marysvale Volcanic Field and its relation to other igneous centers in Utah and Nevada, in *Laccolithic Complexes of Southeastern Utah: Time of Emplacement and Tectonic Setting—Workshop Proceedings*, edited by J. D. Friedman and A. C. Huffman, *U.S. Geol. Surv. Bull.*, *2158*, 167–201.
- Shachak, M., and G. M. Lovett (1998), Atmospheric deposition to a desert ecosystem and its implications for management, *Ecol. Appl.*, *8*, 455–463.
- Swap, R., M. Garstang, S. Greco, R. Talbot, and P. Kallberg (1992), Saharan dust in the Amazon Basin, *Tellus, Ser. B*, *44*, 133–149.
- Van der Hoven, S. J., and J. Quade (2002), Tracing spatial and temporal variations in the sources of calcium in pedogenic carbonates in a semiarid environment, *Geoderma*, *108*, 259–276.
- Vitousek, P. M., M. J. Kennedy, L. A. Derry, and O. A. Chadwick (1999), Weathering versus atmospheric sources of strontium in ecosystems on young volcanic soils, *Oecologia*, *121*, 255–259.
- Vitousek, P. M., O. A. Chadwick, P. Matson, S. Allison, L. Derry, L. Kettley, A. Luers, E. Mecking, V. Monastera, and S. Porder (2003), Erosion and the rejuvenation of weathering-derived nutrient supply in an old tropical landscape, *Ecosystems*, *6*, 762–772.
- Wells, S. G., J. C. Dohrenwend, L. D. McFadden, B. D. Turrin, and K. D. Mahrer (1985), Late Cenozoic landscape evolution on lava flow surfaces of the Cima volcanic field Mojave Desert, California, *Geol. Soc. Am. Bull.*, *96*, 1518–1529.
- Wells, S. G., L. D. McFadden, and J. C. Dohrenwend (1987), Influence of late Quaternary climatic changes on geomorphic and pedogenic processes on a desert piedmont, eastern Mojave Desert, California, *Quat. Res.*, *27*, 130–146.
- Williams, P. E. (1964), Geology, structure, and Uranium deposits of the Moab quadrangle, Colorado and Utah, *U.S. Geol. Surv. Misc. Geol. Invest. Map*, *I-360*, 1:250,000.
- Williams, P. E., and R. J. Hackman (1983), Geology of the Salina Quadrangle, Utah, *U.S. Geol. Surv. Misc. Invest.*, *Map I-591-A*, 1:250,000.
- Wilshire, H. G. (1980), Human causes of accelerated wind erosion in California's desert, in *Thresholds in Geomorphology*, D. R. Coates and J. D. Vitek, pp. 415–433, Allen and Unwin, London.
- Yaalon, D. H., and E. Ganor (1973), The influence of dust on soils during the Quaternary, *Soil Sci.*, *116*, 146–155.

H. L. Goldstein, M. C. Reheis, R. L. Reynolds, and J. C. Yount, Denver Federal Center, U.S. Geological Survey, MS-980, Box 25046, Denver, CO 80225, USA. (hgoldstein@usgs.gov)

J. C. Neff, Geological Sciences and Environmental Studies Departments, University of Colorado, Boulder, CO 80309, USA.